International Journal of Refrigeration 95 (2018) 182–188

Contents lists available at ScienceDirect

International Journal of Refrigeration

journal homepage: www.elsevier.com/locate/ijrefrig

Contact angle measurement for LiBr aqueous solutions on different surface materials used in absorption systems

Asier Martinez-Urrutia[a,*], Peru Fernandez de Arroiabe[b], Miguel Ramirez[a], Manex Martinez-Agirre[b], M. Mounir Bou-Ali[b]

[a] Tecnalia, Energy and Environment Division, Area Anardi, 5, Azpeitia, Gipuzkoa E20730, Spain
[b] Mondragon Unibertsitatea, Faculty of Engineering, Mechanical and Industrial Production, Loramendi 4, Mondragon, Gipuzkoa 20500, Spain

ARTICLE INFO

Article history:
Received 16 November 2017
Revised 24 May 2018
Accepted 27 May 2018
Available online 6 June 2018

Keywords:
Contact-angle
Sessile-drop-test
Absorption technologies
Falling-film
Wetting

ABSTRACT

Wetting surface is a very important issue for the design of absorption applications and heat exchangers. The contact angle is deemed essential in wettability studies; However, LiBr aqueous solution contact angle studies are limited. This work analyses the contact angle of LiBr aqueous solution in the range of 0–55% mass fraction on different material surfaces: copper, aluminum, stainless-steel and polytetrafluoroethylene (PTFE) under atmospheric conditions. A sessile drop technique was used for measuring the contact angles, and a linear relation between solution surface tension and contact angle is observed in the tested materials. The study of three metals show hydrophilic performance ($\theta < 90°$), whereas the PTFE shows hydrophobic performance. Additionally, the effect of the selection of the material, and consequent effect on the contact angle, on the minimum wetting rate and film thicknesses is presented under the working conditions of the absorption technologies. From the wettability point of view, the results show that using stainless-steel and aluminum leads to a slightly better performance than a copper made heat exchanger.

Mesure de l'angle de contact pour les solutions aqueuses de LiBr sur différents matériaux de surface utilisés dans les systèmes à absorption

Mots-clés: Angle de contact; Test de la goutte sessile; Technologies d'absorption; Film tombant; Mouillage

1. Introduction

Absorption technologies have recently become more and more attractive, e.g. absorption chillers, absorption heat transformers and liquid desiccant systems (Rivera et al., 2015). One of the most critical component in these technologies is the absorber, where the refrigerant is directly absorbed by a hygroscopic solution (Garimella, 1999). The falling film configuration is usually used for water–LiBr heat exchangers, due to the large vapor-absorbent interface that optimizes both heat and mass transfer. However, ensuring wettability in falling film components is one of the critical aspects, since the heat exchanger energy efficiency is strongly affected by this parameter. A large effort in order to understand and optimize the performance of the falling film components has been done in the last years, e.g. analysis of the surface structure (micro and macro) of the tubes (Kim et al., 2003a, 2003b; Park et al., 2003,2004; Kang and Kim, 2006) and heat exchanger configuration, mainly determined by the tube diameter and spacing (Yoon et al., 2008). The heat and mass transfer improvements in these studies was directly attributed to the improvement of the tube's wettability. Even the use of hydrophilic coatings has been analyzed by different authors: Yoon et al. 2002 observed that the wetted area of the bundle increased between 110% and 30% when a plasma treated tube was used; an improvement of the wetted

* Corresponding author.
E-mail address: asier.martinez@tecnalia.com (A. Martinez-Urrutia).

https://doi.org/10.1016/j.ijrefrig.2018.05.041

Nomenclature

Symbols

T	— temperature / °C
g	— acceleration of gravity / $m \cdot s^{-2}$

Greek Symbols

Δ	— dimensionless film thickness
δ	— liquid film thickness / mm
Γ	— dimensionless mass flow-rate per unit length
γ	— mass flow rate per unit length / $kg \cdot s^{-1} \cdot m^{-1}$
μ	— dynamic viscosity / $mPa \cdot s^{-1}$
ρ	— density / $kg \cdot m^{-3}$
σ	— surface tension / $mN \cdot m^{-1}$
θ	— contact angle / °
ξ	— solution mass concentration / %

Subscripts

l	— liquid
s	— solid
v	— vapor

Abbreviations

LiBr	— Lithium Bromide
LiCl	— Lithium Chloride
MLFT	— Minimum Liquid Film Thickness
MWR	— Minimum Wetting Ratio
PTFE	— Polytetrafluorethylene

of area by a 30–40% was observed by Qi et al. (2015) when a hydrophilic surface was used. Also the wettability of generators for absorption heat transformers has been visually analyzed (Lazcano-Véliz et al., 2014).

Due to the importance of the wettability analysis, the contact angle is being considered in the absorption technologies studies in the last years. The contact angle measurement is usually considered in surface characterization and wetting studies, being a simple and versatile methodology (Kowk-Yee and Zhao, 2015). Therefore, investigating the contact angle between working fluid and heat exchanger materials is considered crucial, as the contact angle is indispensable for understanding the wetted area. The measurement of the contact angle is being considered in the works of different authors, although it is still limited in the absorption technologies. Qi et al. (2015) studied the contact angle of the commonly used LiCl and LiBr solutions on stainless-steel plates, proposing empirical correlations for the prediction of the contact angle depending on fluid surface tension and solid surface roughness. The author ensures contact angle values, and therefore wettability, is critical for the performance of the falling film components and for the accurate performance prediction of the theoretical models.

The new theoretical researches are including the static contact angle and its influence in the LiBr solution flow spreading over horizontal tube bundles (Ji et al., 2017; Fernandez-Arroiabe et al., 2018) or other configurations, such as over vertical finned plates (Mortazavi et al., 2015). Giannetti et al. (2017) included the effect of partial wetting effect in the mass transfer analytic solution and they observed that the Sherwood number is decreased up to 90% for very low Reynolds numbers when partial wetting is considered. In order to include the effect of the film partial wetting at low Reynolds numbers correlations which, in turn, are dependent on the contact angle are being used.

The aim of this paper is to present the effect of the LiBr concentration, and therefore liquid surface tension, into the contact angle in commonly used absorption technologies materials, copper and stainless-steel, as well as alternative materials proposed by other authors due to corrosion problems, such as aluminum (Romero et al., 2011) and polytetrafluoroethylene (PTFE) (Zhang, 2010). However, wettability issues were not considered in these studies. The obtained results will help in the future development of more accurate heat and mass transfer performance prediction models.

Table 1
Density, temperature and LiBr mass fraction of the tested solutions.

	T / °C	ρ / $kg \cdot m^{-3}$	ξ / w%
Solution 1	23.4	1617.4	55.01
Solution 2	23.0	1442.4	44.10
Solution 3	22.8	1286.0	31.97
Solution 4	23.1	1191.6	23.18
Solution 5 (Distilled water)	22.9	997.6	–

2. Experimental procedure

2.1. Materials

Material samples were prepared by the abrasive polishing process recommended by the Standard Guide for Preparation of Metallographic Specimens (ASTM, 2011). The specimens were cut and installed into a rotating wheel covered with abrasive. Different grinding papers were used from 240 to 1200, finally using 6 μm and 1 μm polishing cloths and diamond paste to obtain smooth and homogeneous surfaces. Cleaning (by ethanol) between stages was required to prevent carryover of abrasives and contamination of subsequent preparation surfaces grinding discs or cloths for fine grinding. Five specimens were prepared for each material, and the selected materials were as follows:

1. Copper (Cu-ETP 99.9);
2. Aluminum (6063-T5);
3. Stainless-Steel (AISI 316 L);
4. PTFE.

The surface roughness has a strong influence on the values of contact angles and, thus, on the wettability.The R_a, R_z and R_q values were below 0.01 μm, 0.11 μm and 0.02 μm in the case of the three metal analyzed and below 0.14 μm, 1.78 μm and 0.22 μm for the PTFE.

2.2. Wet drop tests

Five different LiBr solution concentrations, including water (0% Solution), were tested. Solutions were prepared using commercial LiBr solution provided by Leverton-Clarke (CAS Number: 7550-35-8). Density and temperature of the solutions were measured by an Anton Paar DMA 35 density-meter, while concentrations, presented in Table 1, were calculated by the correlation proposed by Patek and Klomfar (2006).

The contact angle was measured by the static sessile drop method, using an OCA 15plus goniometer (Neurtek Instruments), with an image resolution of 752×582 pixels, 50 fps video recorder and $\pm 0.1°$ accuracy. The drop volume was 3.0 μl, and measurements were performed in a controlled temperature and humidity ambient (23 °C and 45%). The equipment allows monitoring of the spreading dynamic contact angles. Once the drop was deposited, the contact angle was reduced by the effect of the spreading. The drop was allowed to stabilize and let it reaching its final static state. This procedure was monitored, and then the drop profile was analyzed. In Fig. 1 the contact angle percentage variation compared to the previous instant contact angle measurement is observed, on one hand for the water and the LiBr 55% and, on the other hand, for the four material analyzed. Due to the higher viscosity,

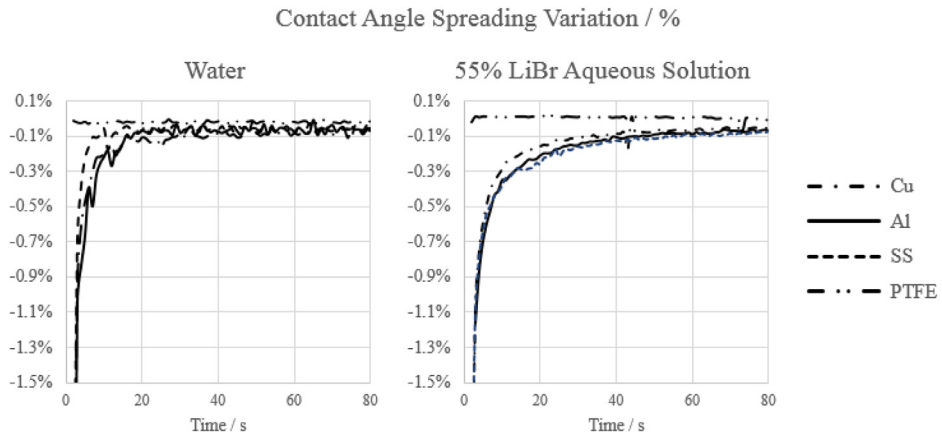

Fig. 1. Wet Drop Test Spreading effect: the percentage variation of the contact angle respect to the previous instant time for the water and 55% LiBr aqueous solution in copper, aluminum, stainless-steel and PTFE.

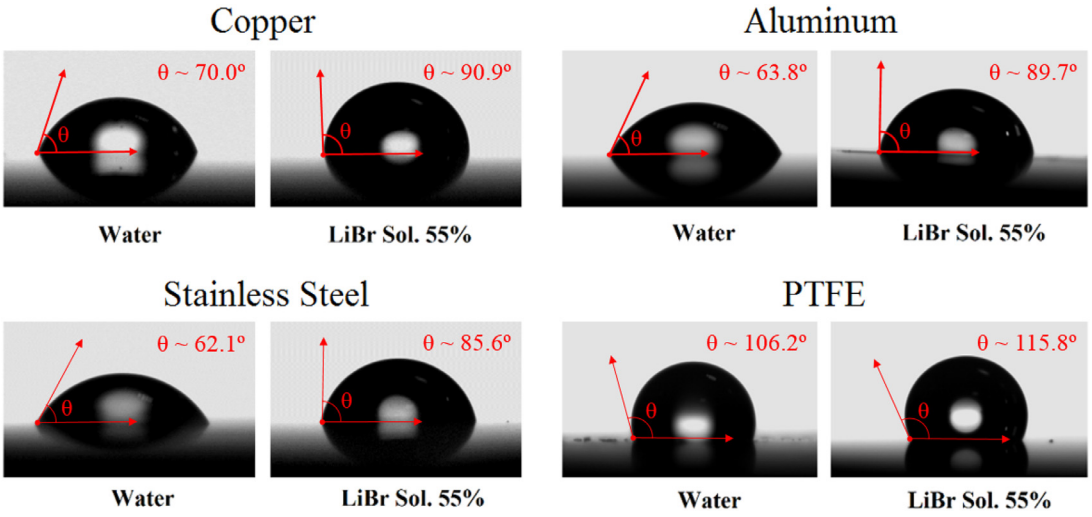

Fig. 2. Water and 55 w% LiBr solution contact angles on copper, aluminum, stainless-steel and PTFE surfaces.

the static state is reached later in the LiBr aqueous solution. As a result of this analysis, the measurement of the contact angle after 60 s from drop deposition was considered, since drop profile changes below 0.1% were observed for the four materials analyzed. This procedure considers dynamic decays to the steady state and the Young contact angle (smooth and chemically heterogeneous surfaces are considered), but by minimization of the evaporation or absorption influence. The measurements of each solution-solid system were repeated over 10 times in different areas of the samples.

3. Results and discussion

3.1. LiBr contact angle in different materials

The surface tension increased with concentration and therefore the contact angle in the four studied materials. Whereas the three metals analyzed showed hydrophilic performance ($\theta < 90°$), PTFE showed hydrophobic performance. For the copper, aluminum and stainless-steel, contact angles were between 70.0° and 90.8°, 62.1° and 85.6° and, 63.8° and 89.7° for water and 55% solution, respectively. For the PTFE surface, contact angles measured were between 106.2° and 115.8°, which the mentioned extreme cases are directly shown in Fig. 2. According to wettability theory, the contact angle is strongly influenced by liquid surface tension (Kowk-Yee and Zhao, 2015). The four materials showed a high linear relation between contact angle and solution surface tension, as shown in Fig. 3, which was calculated by the empirical correlation proposed by Medrano (2001). Fig. 3 shows how the contact angle increased by 1.07, 1.38, 1.45 and 0.53°/mN · m^{-1} for copper, aluminum, stainless-steel and PTFE, respectively.

In Fig. 4, experimental data from Bernett and Zisman (1968) and the experimental contact angles measured on copper and aluminum are compared. Zisman and co-workers proposed the first contact angle interpretation theories studying solid surface excess energy, and they observed that the contact angle, represented by $\cos\theta$, varies smoothly with the liquid surface tension. The data from Bernett and Zisman (1968) was obtained by liquids with surface tensions between 44.00 and 50.80 mN · m^{-1}, but the fluids in this work have surface tensions between 72.28 and 90.83 mN · m^{-1}. The surface tension of the fluids analyzed in these two works are not in the same range, and therefore, they are not directly comparable. However, the linear relation between the $\cos\theta$ and the surface tension reported by Bernett and Zisman (1968) was also observed in the measurements of this work. Thus, the linear relation described by the authors was considered for fitting in the range of the surface tension values of both works. The critical surface tensions obtained by the adjustment proposed in this work, and presented in Fig. 4, were 43.5 mN · m^{-1} (slope of −0.0223 m · mN^{-1}) for copper and 46.8 mN · m^{-1} (slope of −0.0240 m · mN^{-1}) for aluminum, they are in good agreement with values calculated by Bernett and Zisman (1968).

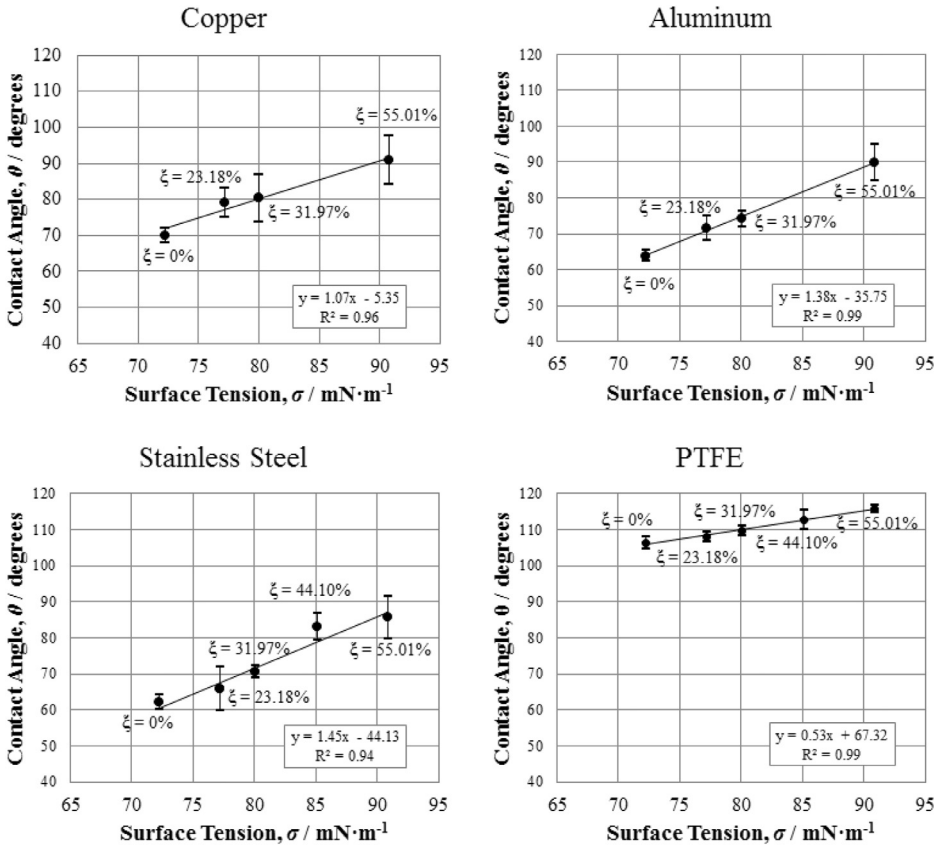

Fig. 3. Effect of the water and LiBr solution surface tension on the contact angle on copper, aluminum, stainless-steel and PTFE. Ambient temperature and humidity: 23 °C and 45%.

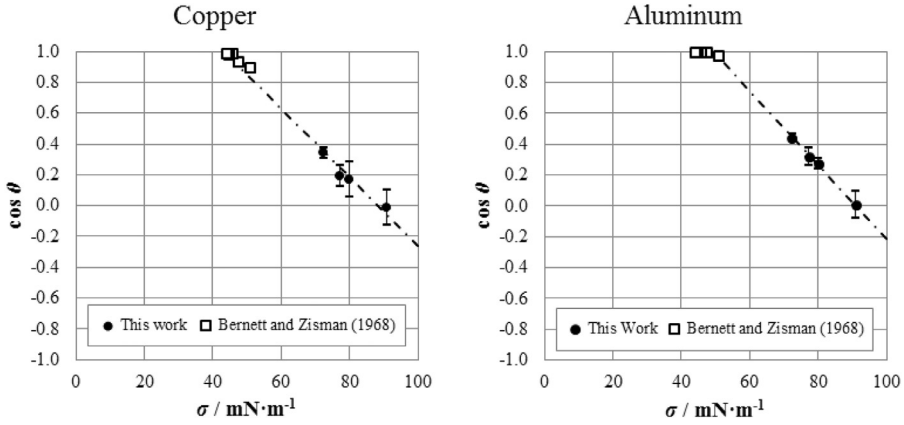

Fig. 4. Cooper and aluminum Zisman Plot ($\cos\theta$ vs. liquid vapor surface tension). Comparison of the experimental contact angles and those presented by Bernett and Zisman (1968).

Experimental results presented by Bueno (2005) were used in the case of the stainless-steel. The surface tension of the liquids used by the author were between 48 $mN \cdot m^{-1}$ (Ethylene Glycol) and 72.8 $mN \cdot m^{-1}$ (Water). However, direct comparison in water shows a deviation of −8.7%. The linear relation between the contact angle $\cos\theta$ and surface tension is observed by combination of the results in both works, and the linear function was adjusted in the range of the surface tension (see Fig. 5), A critical surface tension of 39.5 $mN \cdot m^{-1}$ (slope of $-0.01782\ m \cdot mN^{-1}$) was calculated.

Finally, results obtained in PTFE were compared. In this case, the range of the liquid surface tension studied in this work moves away from the linear relation described by Zisman method. According to Kowk-Yee and Zhao (2015), this is "attributable to H-bonding and polar interactions between the liquid and the solid surface". Fig. 6 shows that the results obtained by this work and data presented by Li and Neumann (1992) and Kwok et al. (1995). Analyzed surface tensions were not in the same range and were not directly comparable. Except water, the results in this work present a contact angle deviation of −4.8% comparing with the results from Li and Neumann (1992). For this reason, data was adjusted to the equation of states described by Kwok and Neumann (1999): Modified Berthelots rule (Eq. (1)) and Alternative Formulation (Eq. (2)):

Modified Berthelots rule:

$$\cos\theta_Y = -1 + 2\sqrt{\frac{\sigma_{sv}}{\sigma_{lv}}}e^{-\beta(\sigma_{lv}-\sigma_{sv})^2} \quad (1)$$

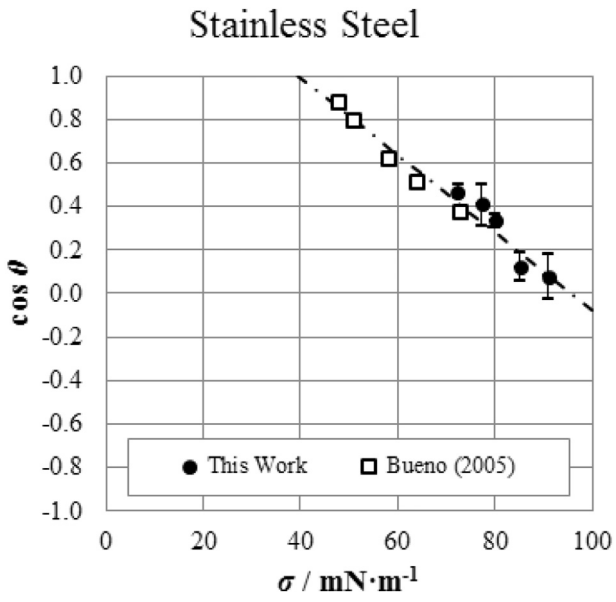

Fig. 5. Stainless-steel Zisman Plot ($\cos\theta$ vs. liquid vapour surface tension). Comparison of the experimental contact angles and those by Bueno (2005).

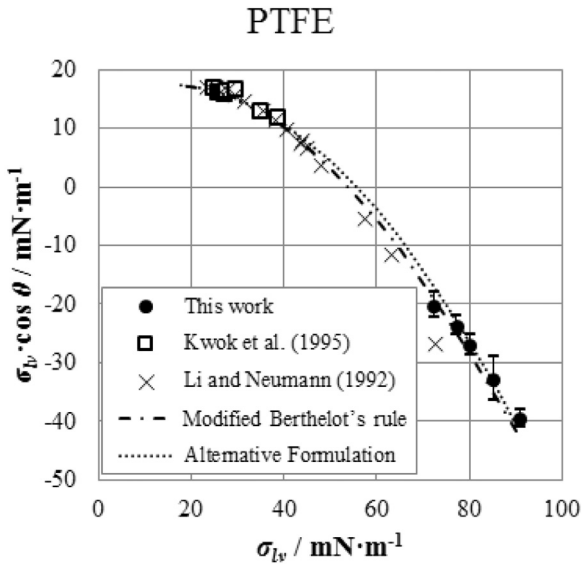

Fig. 6. $\sigma_{lv}\cdot\cos\theta$ vs. σ_{lv} for present experimental results and data from Li and Neumann (1992) and Kwok et al. (1995). Adjusted Modified Berthelots Rule and Alternative Formulation.

Alternative Formulation:

$$\cos\theta_Y = -1 + 2\sqrt{\frac{\sigma_{sv}}{\sigma_{lv}}} - \beta_1(\sigma_{lv}-\sigma_{sv})^2 \tag{2}$$

where θ_Y is the ideal Young contact angle, σ_{lv} and σ_{sv} are the liquid–vapour and solid–vapour inter-facial tensions, respectively, and β and β_1 are constants to be adjusted. Solid–vapour tensions of 17.2 and 17.3 $mN\cdot m^{-1}$ were obtained by Modified Berthelot and Alternative formulations, respectively. Values obtained by Kwok et al. (1995) were 18.0 and 17.8 $mN\cdot m^{-1}$, respectively. Therefore, results obtained in this work are considered in of β=0.0000924 $(m\cdot mN^{-1})^2$ and β_1=0.0000710 $(m\cdot mN^{-1})^2$ were obtained by this least-square analysis (Kwok et al., 1995).

3.2. Effect of the material selection in the minimum wetting rate

Results obtained in this work have been used to study the effect of the use of different materials in the minimum wetting rate (MWR) and therefore in the design of the heat exchangers of the absorption technologies. MWR is defined as the lowest flow rate needed to ensure that the surface remains covered by a continuous thin liquid film, which directly depends on the wettability performance and on the contact angle. Different analytic expressions has been proposed in the bibliography (Hartley and Murgatroyd, 1964; Hobler, 1964; Mikielewicz and Moszynskl, 1976; Doniec, 1991; El-Genk and Saber, 2001). A comparison of different authors expressions and experimental works are presented in Fig. 7.

In this work, expressions proposed by El-Genk and Saber (2001) for predicting the minimum liquid film thickness (MLFT) and the MWR were used. These MWR-Contact angle and MLFT-Contact angle relations, which are based on the minimum total energy show the best agreement with the experimental data from Ponter et al. (1967) and Munakata et al. (1975), as shown in Fig. 7.

The author calculates MLFT, Δ_{min}, as follows:

$$\Delta_{min} = (1-\cos\theta)^{0.22} \tag{3}$$

And then MWR, Γ_{min}, may be calculated by the following empirical correlation:

$$\Gamma_{min} = 0.67\cdot\Delta_{min}^{2.83} + 0.26\cdot\Delta_{min}^{9.51} \tag{4}$$

Where dimensionless flow rate and dimensionless film thickness are defined as follows:

$$\Delta = \delta\cdot\left(\frac{g}{\rho\mu\sigma^3}\right)^{\frac{1}{5}} \tag{5}$$

$$\Gamma = \gamma\cdot\left(\frac{\rho^3 g^2}{15\mu^2\sigma}\right)^{\frac{1}{5}} \tag{6}$$

In this MWR and MLFT study, performance parameters, i.e., absorber and generator inlet and outlet temperature and solution concentration, proposed by Herold et al. (2016) for both absorption chillers and absorption heat transformers were considered. First, for both proposed cycles, average solution temperature and concentration were considered, and then density, viscosity and surface tension were calculated by correlations proposed by Patek and Klomfar (2006) and Medrano (2001). Second, contact angles for each component depending on possible materials were predicted (by use of the results presented in Fig. 3). Finally, these contact angles were used to calculate the minimum film thickness according to Eq. (3) and the minimum solution flow rate by Eq. (4) to ensure fully and continuously wet surface, which the results are presented in Table 2.

According to the results obtained in this study, angles obtained on aluminum and stainless-steel surfaces are lower than the angles obtained on copper surfaces. These differences become greater when higher temperature applications are required, reducing contact angles between 1.98 and 6.04% in the case of the aluminum and between 4.06% and 9.24% in the case of stainless-steel. Results in Table 2 show that due to the improved wettability of aluminum and stainless-steel, lower mass flow rates per unit length, and therefore lower film thicknesses, would be needed in these materials to obtain a uniform film similar to the film on copper. The specific mass flow rates for the copper would lied between 0.1328 and 0.2293 $kg\cdot s^{-1}\cdot m^{-1}$ for the absorbers in the Heat Transformer and the Chiller respectively, which are the studied components with highest and lowest working temperatures. These flow rates would be reduced to 0.1203 and 0.2220 $kg\cdot s^{-1}\cdot m^{-1}$ if the heat exchanger would be made of aluminum, and to 0.1139 and 0.2144 $kg\cdot s^{-1}\cdot m^{-1}$ if stainless-steel is considered. The lower flow

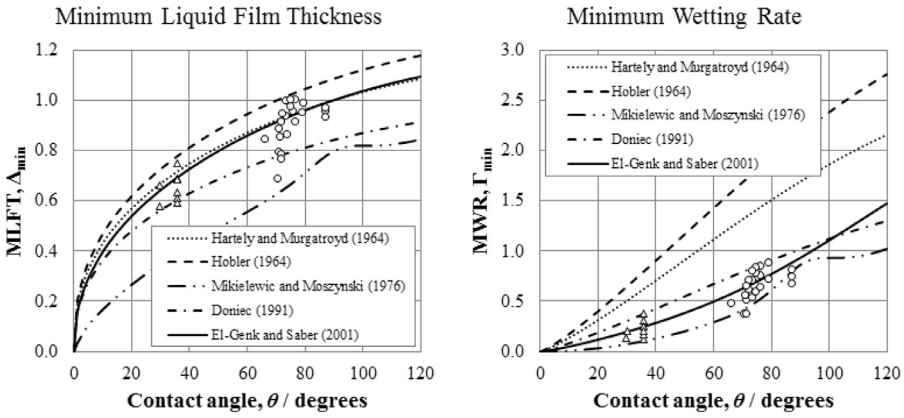

Fig. 7. Comparison of MLFT and MWR prediction expressions and data for water (O-points, from Ponter et al. (1967) and glycerol–water mixtures (Δ-points, from Munakata et al. (1975).

Table 2
Prediction of the contact angle and minimum wetting rate and liquid film thickness for copper, aluminum, stainless-steel and PTFE depending on the falling film heat exchanger operating conditions.

	Single-Effect AbsorptionChiller (Type I)				Single-Effect Heat Transformer (Type II)			
	Absorber		Generator		Absorber		Generator	
	inlet	outlet	inlet	outlet	inlet	outlet	inlet	outlet
T / °C	44.96	32.72	63.61	89.36	164.01	153.90	102.41	111.60
ξ / w%	62.16	56.48	56.48	62.16	63.32	59.44	59.44	63.99
Average properties:								
ρ / kg·m^{-3}	1693.06		1674.21		1666.87		1704.70	
μ / mPa·s^{-1}	5.09		2.72		1.29		2.19	
σ / mN·m^{-1}	92.11		88.72		82.02		87.66	
Copper*								
θ / °	93.20		89.58		82.41		88.45	
MWR, Γ_{min}	0.9844		0.9229		0.8068		0.9041	
γ_{min} / kg·s^{-1}·m^{-1}	0.2293		0.1850		0.1328		0.1730	
MLFT, Δ_{min}	1.0120		0.9984		0.9693		0.9940	
δ_{min} / mm	0.6055		0.4645		0.3303		0.4185	
Aluminum								
θ / °	91.35	−1.98%	86.68	−3.24%	77.44	−6.04%	85.22	−3.65%
MWR, Γ_{min}	0.9528	−3.20%	0.8750	−5.19%	0.7308	−9.42%	0.8514	−5.83%
γ_{min} / kg·s^{-1}·m^{-1}	0.2220		0.1754		0.1203		0.1629	
MLFT, Δ_{min}	1.0052	−0.68%	0.9869	−1.14%	0.9475	−2.25%	0.9810	−1.30%
δ_{min} / mm	0.6013		0.4592		0.3228		0.4130	
Stainless-Steel								
θ / °	89.42	−4.06%	84.51	−5.66%	74.80	−9.24%	82.98	−6.18%
MWR, Γ_{min}	0.9203	−6.51%	0.8400	−8.99%	0.6921	−14.22%	0.8157	−9.78%
γ_{min} / kg·s^{-1}·m^{-1}	0.2144		0.1684		0.1139		0.1561	
MLFT, Δ_{min}	0.9978	−1.41%	0.9781	−2.03%	0.9353	−3.51%	0.9717	−2.24%
δ_{min} / mm	0.5969		0.4551		0.3187		0.4091	
PTFE								
θ / °	116.14	24.61%	114.34	27.65%	110.79	34.44%	113.78	28.64%
MWR, Γ_{min}	1.3989	42.11%	1.3658	48.00%	1.3004	61.18%	1.3555	49.93%
γ_{min} / kg·s^{-1}·m^{-1}	0.3259		0.2739		0.2141		0.2593	
MLFT, Δ_{min}	1.0836	7.07%	1.0789	8.06%	1.0691	10.29%	1.0774	8.39%
δ_{min} / mm	0.6483		0.5020		0.3643		0.4536	

* Reference

rates in the aluminum and stainless-steel would result in thinner film thicknesses, reducing from coppers 0.3303–0.6055 mm thickness to 0.3228–0.6013 for aluminum and between 0.3187 and 0.5969 for stainless-steel. Flow rates would be reduced between 3.20% and 9.42% if the aluminum would be selected instead of copper, while film thickness would be reduced between 0.68% and 2.25%. If stainless-steel is considered, the minimum required flow rate would be reduced between 4.06% and 9.24%, consequently reducing film thickness between 1.41% and 3.51%. Thinner stable films would be favorable in absorption and desorption processes, since absorption mass fluxes would be greater resulting in an increase of the capacity and a higher efficiency of the components (Giannetti et al., 2017).

On the other hand, PTFE contact-angle tests showed hydrophilic performance, and this would result in worse falling-film heat-exchanger performance, as shown in Table 2. The predicted contact angles for the selected working conditions would be increased between 24.61% and 34.44% compared to those obtained in copper. Therefore, the flow rates and film thicknesses required to obtain a uniform wet PTFE surface would be increased to 0.2141–0.3259 kg·s^{-1}·m^{-1} and 0.3643–0.6483 mm, i.e. between 42.11% and 61.48% and 7.07% and 10.29%, respectively; and this would

result, from a wettability perspective (not considering also worse thermal conductivity), in a much lower efficient heat exchanger, than those made of copper, aluminum or stainless-steel.

4. Conclusions

The contact angle of the aqueous LiBr solutions with different concentrations up to 55% on copper, aluminum, stainless-steel and PTFE have been measured by sessile drop tests. As a result of the performed tests, a straight-linear relation between the contact angle and the solution surface tension, depending on the LiBr concentration, is observed. Copper, aluminum and stainless-steel show a hydrophilic performance, while PTFE showed hydrophobic performance. Contact angles on the three metals tested were between 70.0° and 90.8° on copper, between 62.1° and 85.6° on aluminum and 63.8° and 89.7° on stainless-steel for water and 55% solution, respectively. The critical solid surface tension of the copper, aluminum and stainless-steel was calculated by these results, together with the data available in previous research. Critical surface tensions of 44, 45 and 39.5 $mN \cdot m^{-1}$ were determined for copper, aluminum and stainless-steel, respectively. In contrast, contact angles measured in the PTFE ranged between 106.2° and 115.8°. Besides, the solid surface tension of the PTFE was calculated by adjusting the modified the modified Berthelots rule and the alternative formulation. Solid-vapour tensions of 17.2 and 17.3 $mN \cdot m^{-1}$ were obtained by Modified Berthelot and Alternative formulations, respectively. Results obtained in this study are in good agreement with those in previous research.

In addition, an estimation of the minimum wetting rate and the minimum film thickness to obtain a wetted uniform surface in the components composing an absorption chiller and an absorption heat transformer has been performed. By combining the wettability studies related to the contact angle and different components under typical working conditions, the required minimum wetting rates and minimum solution film thicknesses to ensure a complete wetting on different materials were calculated and quantitatively compared to copper as the usually considered material. Aluminum and stainless-steel showed very similar performances but resulted in slightly better wetting performances compared to the performance obtained by copper, which results in greater mass transfer fluxes and more efficient heat exchangers.

Wettability is considered crucial in the design of falling film heat exchangers, but, data in contact angles is still limited for LiBr aqueous solutions. Consequently, results obtained in this work may also help in the future designs when wettability aspects are considered.

Acknowledgment

The authors would like to thank the support of the project Indus3Es: Industrial Energy and Environmental Efficiency funded by the Horizon 2020 framework of the European Union, Project No. 680738. The authors would also like to express their gratitude for the support of MICRO4FAB and BEROA–GO 3.0 and Research Groups (No. IT009-16).

References

ASTM, 2011. E3-11 Standard Guide for Preparation of Metallographic Specimens 1. ASTM Copyright, 1–12. 10.1520/E0003-11.2

Bernett, M.K., Zisman, W., 1968. Effect of adsorbed water on the critical surface tension of wetting on metal surfaces. J. Colloid Interface Sci. 28 (2), 243–249.

Bueno, H., 2005. The Critical Surface Tension of 316L Stainless Steel. Master's Thesis. Paper 2728, 2005. San Jose State University.

Doniec, A., 1991. Laminar flow of a liquid rivulet down a vertical solid surface. J. Chem. Eng. 69 (1), 198–202.

El-Genk, M.S., Saber, H.H., 2001. Minimum thickness of a flowing down liquid film on a vertical surface. Int. J. Heat Mass Transf. 44, 2809–2825.

Fernandez-Arroiabe, P., Martinez-Urrutia, A., Peña, X., Martinez-Agirre, M., Bouali, M., 2018. Influence of the contact angle on the wettability of horizontal-tube falling films in the droplet and jet flow modes. Int. J. Refrig.. Accepted Manuscript. Available online.

Garimella, S., 1999. Miniaturized heat and mass transfer technology for absorption heat pumps. In: Proceedings of the International Sorption Heat Pump Conference, Munich, Germany, pp. 661–670.

Giannetti, N., Rocchetti, A., Yamaguchi, S., Saito, K., 2017. Analytical solution of film mass-transfer on a partially wetted absorber tube. Int. J. Therm. Sci. 118, 176–186.

Hartley, D., Murgatroyd, W., 1964. Criteria for the break-up of thin liquid layers flowing isothermally over solid surfaces. Int. J. Heat Mass Transf. 7 (9), 1003–1015.

Herold, K.E., Radermacher, R., Klein, S.A., 2016. Absorption Chillers and Heat Pumps. CRC press. ISBN-13: 978-1-4987-1435-8

Hobler, T., 1964. Minimum surface wetting. Chem. Stosow. B 2, 145–159.

Ji, G., Wu, J., Chen, Y., Ji, G., 2017. Asymmetric distribution of falling film solution flowing on hydrophilic horizontal round tube. Int. J. Ref. 78, 83–92.

Kang, Y.T., Kim, J.-K., 2006. Comparisons of mechanical and chemical treatments and nano technologies for absorption applications. HVAC & R Res. 12 (S2), 807–819.

Kim, J.K., Park, C.W., Kang, Y.T., 2003a. Wettability correlation of microscale hatched tubes for falling film absorption application. J. Enhanc. Heat Transf. 10 (4).

Kim, J.K., Park, C.W., Kang, Y.T., 2003b. The effect of micro-scale surface treatment on heat and mass transfer performance for a falling film H_2O/LiBr absorber. Int. J. Refrig. 26 (5), 575–585.

Kowk-Yee, L., Zhao, H., 2015. Surface Wetting Characterization, Contact Angle, and Fundamentals.. Springer. ISBN 978-3-319-25212-4

Kwok, D., Budziak, C., Neumann, A., 1995. Measurements of static and low rate dynamic contact angles by means of an automated capillary rise technique. J. Colloid Interface Sci. 173 (1), 143–150.

Kwok, D.Y., Neumann, A.W., 1999. Contact angle measurement and contact angle interpretation. Adv. Colloid Interface Sci. 81 (3), 167–249.

Lazcano-Véliz, Y., Siqueiros, J., Juárez-Romero, D., Morales, L., Torres-Merino, J., 2014. Analysis of effective wetting area of a horizontal generator for an absorption heat transformer. Appl. Therm. Eng. 62 (2), 845–849.

Li, D., Neumann, A., 1992. Contact angles on hydrophobic solid surfaces and their interpretation. J. Colloid Interface Sci. 148 (1), 190–200.

Medrano, M., 2001. Development of an air-cooled vertical tube absorber for an absorption air conditioner using waterlithium bromide. University of Tarragona, Spain Ph.D. thesis.

Mikielewicz, J., Moszynskl, J., 1976. Minimum thickness of a liquid film flowing vertically down a solid surface. Int. J. Heat Mass Transf. 19 (7), 771–776.

Mortazavi, M., Isfahani, R.N., Bigham, S., Moghaddam, S., 2015. Absorption characteristics of falling film Libr (lithium bromide) solution over a finned structure. Energy 87, 270–278.

Munakata, T., Watanabe, K., Miyashita, K., 1975. Minimum wetting rate on wetted-wall column. J. Chem. Eng. 8 (6), 440–444.

Park, C.W., Cho, H.C., Kang, Y.T., 2004. The effect of heat transfer additive and surface roughness of micro-scale hatched tubes on absorption performance. Int. J. Refrig. 27 (3), 264–270.

Park, C.W., Kim, S.S., Cho, H.C., Kang, Y.T., 2003. Experimental correlation of falling film absorption heat transfer on micro-scale hatched tubes. Int. J. Refrig. 26 (7), 758–763.

Patek, J., Klomfar, J., 2006. A computationally effective formulation of the thermodynamic properties of LiBr–H_2O solutions from 273 to 500k over full composition range. Int. J. Refrig. 29 (4), 566–578.

Ponter, A., Davies, G., Ross, T., Thornley, P., 1967. The influence of mass transfer on liquid film breakdown. Int. J. Heat Mass Transf. 10 (3), 349–352.

Qi, R., Lu, L., Jiang, Y., 2015. Investigation on the liquid contact angle and its influence for liquid desiccant dehumidification system. Int. J. Heat Mass Transf. 88, 210–217.

Rivera, W., Best, R., Cardoso, M., Romero, R., 2015. A review of absorption heat transformers. Appl. Therm. Eng. 91, 654–670.

Romero, R., Esparza, S. H., García, D. H., Castañeda, E. I., 2011. Cuantificación de la corrosión de Aluminio Expuesto a un Fluido Usado en Bombas de Calor avanzadas y Convencionales (in Spanish). Universidad Autónoma del Estado de Morelos. Mexico.

Yoon, J.I., Kim, E., Choi, K., Seol, W., 2002. Heat transfer enhancement with a surfactant on horizontal bundle tubes of an absorber. Int. J. Heat Mass Transf. 45 (4), 735–741.

Yoon, J.I., Phan, T.T., Moon, C.-G., Lee, H.-S., Jeong, S.-K., 2008. Heat and mass transfer characteristics of a horizontal tube falling film absorber with small diameter tubes. Heat Mass Transf. 44 (4), 437–444.

Zhang, X.D., 2010. Comparison and analysis of lithium bromide–water absorption chillers using plastic heat transfer tubes and traditional lithium bromide–water absorption chillers. Int. J. Mech., Aerosp., Ind., Mechatron. Manuf. Eng. 4 (5), 424–427.